Egypt. J. Chem. **Vol. 68**, No. 12 pp. 55 - 67 (2025)

Egyptian Journal of Chemistry

http://ejchem.journals.ekb.eg/

Synthesis, Td-Dft Calculations and Dyeing Properties of New Hybrid Blend Anthraquinone Polymeric Dye for Dyeing Polyester Fiber

El-Refaie S. Kenawy[a], Sherif M. Bekhet[a], Mohamed E. Sadek[a], Ahmed F. Al-Hossainyb*, Hany Kafafy[c]

[a]*Polymer Research Group, Department of Chemistry, Faculty of Science, Tanta University, Tanta 31527, Egypt*

[b] *Chemistry Department, Faculty of Science, New Valley University, El-Kharga 72511, New Valley, Egypt*

[c]*Dyeing, Printing and Textile Auxiliaries Department, Textile Research and Technology Institute, National Research Centre, 33 El-Behouth St, Dokki, P.O. 12622, Giza, Egypt*

Abstract

This study explores the synthesis, theoretical calculations, and dyeing properties of a novel hybrid blend anthraquinone polymeric dye designed for polyester fiber dyeing applications. An innovative blue polymeric dye (PAA+AnD) HB hybrid blend was produced by reacting anthraquinone dispersion Blue 56 dye (AnB56) with polyacrylic acid (PAA). This polymeric dye was confirmed by 1HNMR, elemental analysis, FTIR, UV visible spectrophotometry, SEM, and EDX analysis. The produced polymeric dye was used to color polyester fabric in large quantities. Using Hartree-Fock (HF) and density functional theory (DFT-B3LYP), the ideal geometries, vibrational wavenumbers, vibrational band intensities, and various atomic charges of 9VC have been examined. The new anthraquinone-based polymeric dye was synthesized through a stepwise chemical process, incorporating both anthraquinone moieties and polymeric segments to enhance the dye's stability and performance. Time-dependent density functional theory (TD-DFT) calculations were employed to investigate the electronic properties, absorption spectra, and excited-state dynamics of the synthesized dye molecules. The results revealed significant insights into the dye's photophysical behaviour, providing a deeper understanding of its light absorption and electron transfer processes. The dyeing efficiency, color fastness, and overall performance of the hybrid polymeric dye were evaluated on polyester fibers, demonstrating superior dye uptake, vibrant coloration, and excellent wash and light fastness properties. This study highlights the potential of anthraquinone-based polymeric dyes for advanced textile applications, offering an environmentally friendly and effective solution for polyester dyeing.

Keywords: Nanoblend, TD-DFT calculations, PET, poly acrylic acid, Disperse blue 56 dye, polyester fiber, qualities of fastness.

1. Introduction

Disperse dyes are colored organic compounds with a low molecular weight and low water solubility.They can be used to color hy drophobic fibers likenylon, polyester, polypropylene, and cellulose acetate from an aqueous dispersion.A wide range of disperse dyes, most of which haveimproved in fastness and application over previousdyes, were introduced in the last ten years and wereu sed to color polyester.The use of polymeric dye as a new and useful dyeing technique was one of these developments.When dyes are chemically integrated into the mainside chains of polymers, a new type of dye known as polymeric dyes is produced.The char acteristics of polymers and dyes are combined in polymeric dyes.Another advantage of polymeric colorants is the ability to modify a range of physical characteristics, such as solubility, absorption, migration, and viscosity. They don't sublime and are typically nonabrasive and low in toxicity. The merging of color and polymer chemistry could potentially offer a larger choice of goods. By grafting anthraquinone dyes onto high molecular materials, we intend to utilize their advantages to produce polymeric dyes [14].[23]. Dyes adhering to polyacrylic acid: As a polyelectrolyte, polyacrylic acid may interact with charged dyes such as Blue 56. The charged groups of the dye molecules can establish electrostatic contacts with the carboxylate groups in PAA [18]. The dye may adsorb onto the PAA polymer as a result of this electrostatic attraction, producingDye-polymercomplex formation.Moreover, there's another advantage of polymeric colorants is the capacity to modify a range of physical characteristics, such as solubility, absorption, migration, and viscosity. They don't sublime and are typically nonabrasive and low in toxicity. Combining color with polymer chemistry may result in a greater selection of goods. By grafting anthraquinone dyes onto high molecular materials, we intend to utilize their advantages to produce polymeric dyes [14].[23]. Dyes adhering to

*Corresponding author e-mail: ahmed73chem@nvu.edu.eg;.; (Ahmed F. Al-Hossainyb).
Received date 04 December 2024; Revised date 03 February 2025; Accepted date 04 February 2025
DOI: 10.21608/ejchem.2025.137315.10933

polyacrylic acid: As a polyelectrolyte, polyacrylic acid may interact with charged dyes such as Blue 56. The charged groups of the dye molecules can establish electrostatic contacts with the carboxylate groups in PAA [18]. The dye may adsorb onto the PAA polymer as a result of this electrostatic attraction.

In order to design and synthesize new, high-performing dye sensitizers and to shed light on the relationship between structures, properties, and performance, theoretical investigations of the physical features of dye sensitizers are therefore crucial. Recently, a hybrid blend (PAA+AnB56)HB/Iso was created and produced. It has an anchoring carboxyl group and an electron-donor-acceptor moiety in its α-conjugated oligo-tetrahydro quinoxaline unit [6]. The border molecular orbitals were also determined using B3LYP/6-31+G(d) [19–13]. Which dyes have different electronic structures and absorption properties between (AnB56)HB/Isoand (PAA+AnB56)HB/Iso. Time-dependent DFT (TD-DFT) calculations and density functional theory (DFT) were used to analyze the electronic absorption spectra and investigate the dye's geometry, electronic structures, polarizabilities, and hyperpolarizabilities in order to answer the question and comprehend the sensitized mechanism.

Therefore, theoretical research on the physical properties of dye sensitizers is crucial for both creating and synthesizing novel, high-performing dye sensitizers and shedding light on the relationship between structures, performance, and attributes. PAA+AnB56)HB/Iso is a hybrid blend that was newly created and synthesized. Its α-conjugated oligo-tetrahydro quinoxaline unit has an electron-donor-acceptor moiety, along with an anchoring carboxyl group [6]. Additionally, B3LYP/6-31+G(d) was used to identify the border molecular orbitals [19–13]. Which dyes, (AnB56)Iso and (PAA+AnB56)HB/Iso, differ from one another in terms of their absorption properties and electronic structures? The electronic absorption spectra were examined, along with the dye's geometry, electronic structures, polarizabilities, and hyperpolarizabilities, using density functional theory (DFT) and time-dependent DFT (TD-DFT) calculations to answer the question and comprehend the sensitized mechanism.

This study created a hybrid blend of polymeric dye based on anthraquinone. The chemical structure of the generated polymeric dye was ascertained by means of FT-IR, 1H NMR, SEM, and EDX analysis. The color performance and adsorption properties of the generated polymeric dyes and anthraquinone dye have been tested and compared using UV-Vis absorption spectra. The values discovered through experimentation are reasonably consistent with the structural properties predicted in TD-DFT by DMOl3/CASTEP.

2. Experimental

2.1. Materials and methods

Chemicals used were commercially available and were used without further purification.All reagents and solvents were of commercial grade.

2.2. Instruments

2.2.1. The method of dying

2.2.2. The KMS-IR lab dyeing machine (China) was the one used in this project. Because it is heated by infrared radiation, it is not contaminated by polyethylene glycol and may be used to dye a variety of textiles and yarns. Simply remembering the program number that has been stored for dyeing is the operation. The dye tubes are easy to plug and remove. Because of the design of the dyetube lid, introducing chemicals throughout the dying process doesn't require opening the dye tube.

2.2.3. Characterization

FTIR for monomeric and polymeric dyes was recorded on a disk with KBR (BRUKER) using FTIR-4000. UV-Vis spectrophotometry analysis was carried out using color matching system Konica Minolta (Japan) apparatus with I.C.S company software (Italy) and the spectrophotometer software based on The CIELAB color space system that represents quantitative relationship of color on three axes (L* value indicates lightness, a* and b* are chromaticity coordinates where the a* value indicates red-green components of color, while the yellow and blue components are represented on the b* axis. The elemental analyzer examined the polymeric dye's elemental analysis. Varian MercuryVX-300 1H NMR spectrometer was used to evaluate the nuclear magnetic resonance. 1H spectra were recorded at 75.46 MHz in dimethyl sulfoxide (DMSO-d6). Chemical shift quoted in δ.

2.2.4. Washing Fastness

Washing fastness tester LM (KMS) Company (china) was used for measuring washing fastness. The objective of measuring color fastness to washing is to determine how washing affects the textile's color fastness.

A sample of the dyed fabric is placed in contact with one or two designated neighboring fabrics, mechanically shaken in a soap solution for a predetermined amount of time and temperature, rinsed in a vacuum oven, and dried. The grey scale or computer color matching system (ISO105C08/C08/C09 and AATCC61) are used to evaluate the specimen's color shift and the staining of the nearby fabrics [8].

2.2.5. Sublimation fastness.

Sublimation fastness tester SB1 (KMS) Company (China) (Fig. 1b) was used for measuring sublimation fastness which is one of the most important requirement tests of dyed polyester. The migration behavior and wet fastness of the dispersed dye on polyester are closely involved with their response to heat treatment. In general, the Sublimation fastness of disperse dyes is tested for staining and shade shift at 150oC, 180 ^{0}C, and 210 ^{0}C for 30 seconds and the rating is done on 1-5 greyscale according to the standard test method. The method was described in (AATCC test method 117-2004, ISO 105-P01) [27]

2.2.6. Synthesis of hybrid blend organic dye (PAA+AnB56)^{HB}

Under magnetic stirring (0.3 g, 0.82 m mol) of anthraquinone disperse blue56 dye (AnB56)was dissolved in 80 ml distilled water, next the blue dye solution was mixed with 20 milliliters of polyacrylic acid (PAA) and 25 milliliters of water. Sodium carbonate solution (10%, w/w) was used to bring the pH of the solution down to 10-10.5. The mixture was stirred at room temperature (25^{0}C) then the reaction temperature increased to 120^{0}C by heating on a hot plate for 1 hr. The reaction mixture was dried on a vacuum by a rotary evaporator [26-37]. The isolated hybrid blend organic dye was identified using FT-IR, UV-Vis absorption spectra, and ^{1}H-NMR.

2.3. Dyeing Method

2.3.1. Method of dyeing polyester fiber with anthraquinone dye (disperse blue 56 dye) (AnB56)

The dyeing of polyester fiber was done using the procedure outlined previously[25]. A practical lab technique for dying polyester fiber is carried out under high pressure (24–30 psi) and high temperature (130–135°C), utilizing IR high-temperature beaker dyeing machine (Fig. 1). The dye solution was made by adding 100 mL of water to 0.3 g of powdered dye and stirring. Next, 10 mL of the dye suspension that had already been made was added to the reaction mixture along with 1.0 g/L of a dispersing agent.

Finally, the pH was adjusted to 4.5–5 using 40 mL of water and acetic acid. A beaker with a screw cap and a cover was filled with the previously described suspension. After correctly rolling and dropping a wet polyester fiber sample into the beaker, the beaker was closed and placed on the rotating carriage within the tank. After allowing the rotatory carrier to spin, the polyester fiber's temperature was progressively raised to 130°C at a rate of 2°C per minute. Under pressure, the dyeing procedure was carried out for 45 minutes. The beaker was taken out of the rotatory carrier and given a water wash after cooling for one hour. The dyed sample was cleaned in 50°C hot water, then rinsed with cold water and dried in a hot air dryer[24-42].

2.3.2. Method of dyeing polyester fiber with hybrid blend organic dye (PAA+AnB56)^{HB}

The process of dying with hybrid blend organic dye (PAA+AnB56)^{HB} was similar to that described with monomeric dye. (10 mL) was taken off the fine solution (PAA+AnB56)^{HB} and combined with an appropriate dispersing agent and (40 ml) water to a beaker provided with a wetted pattern of polyester fiber was rolled into the beaker. Using acetic acid, the pH of the resultant dispersion solution was brought to 4.5–5. At 130oC, polyester fiber was dyed. Under pressure, the coloring process lasted for 45 minutes. The colored design was taken out and cleaned with cold water before being dried in a hot air dryer after cooling for an hour.

2.4. Fastness Properties

2.4.1. Fastness Test for polyester fiber dyed with anthraquinone dye and hybrid blend organic dye.

The sublimation color fastness teste was done as,first, the sample was prepared where the dyed sample was cut in size (4x10 cm) and the white bleached polyester sample is placed over the fabric to be tested. Next, the sample was placed between two metal plates on a fastness tester that was operated at a moderate pressure and temperature under careful heating control. Heating plates were put down to hot press for 15-30 sec at 150^{0}C temperature. Tested samples were taken out and a grayscale was used to evaluate the discoloration of the original sample and the staining degree of white cloth. The above process was repeated at 180oC and 210^{0}C.

2.4.2. Wash Fastness Test for polyester fiber dyed with anthraquinone dye and hybrid blend organic dye.

The dyed sample was cut in 5×10 cm according to AATCC and put with the multifiber sample run for the necessary amount of time in a wash wheel that contains wash liquor, steel balls, and standard detergent. Next, the sample was taken out, cleaned, and dried[32]. A standard grey scale was employed for evaluation, wherein half steps of grades ranging from 1 to 5 are assigned. The assessment must be completed in a dark room with uniform lightning conditions and in a clean greyscale.

2.5. Methods of Geometry

Using DFT and the Gaussian03 program, this material's polarizability, hyperpolarizability, electronic structure, and geometry of the isolated molecules of (PAA)^{Iso}, (An B56)^{Iso}, and (PAA+AnB56)$^{HB/Iso}$ were determined [15]. We employed the

Lee-Yang-Parr gradient-corrected correlation potential (B3LYP) and Becke's three-parameter exchange potential corrected for gradients (B3LYP) to perform DFT on basis sets of polarized split-valence 6-31G*[22-27-11]. The identification of oscillator strengths and permitted excitations is required to get spectra of electronic absorption. Using the identical basis sets as well as PBE1PBE [33], MPW1PW91[4], and B3LYP hybrid functional, TD-DFT was used to do these calculations.

The polarizable continuum model (PCM) was used in non-equilibrium form to determine the solvent's impact [10] Effective studies of cluster and molecular absorption spectra have been conducted with TD-DFT, including hybrid blend thin film, ethanolic solutions [41] and thiazolopyrimidine derivative in a DMF solution [39].

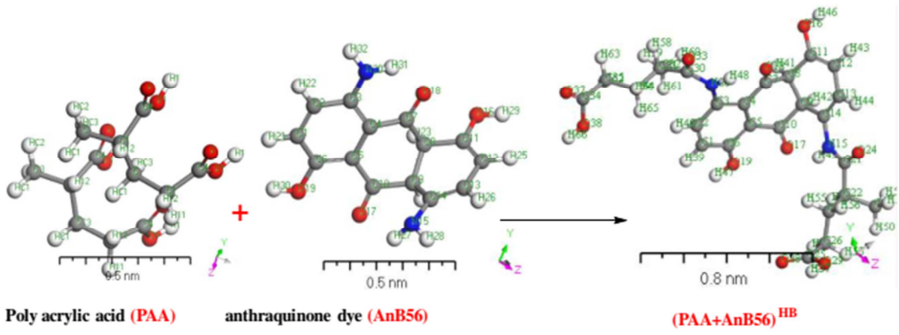

Figure 1: Optimized hybrid blend's geometrical structures $(PAA)^{Iso}$, $(AnB56)^{Iso}$ and $(PAA+AnB56)^{HB/Iso}$. (B3LYP/6-31G*, For clarity, Atoms of hydrogen have been removed. The spheres containing 7, 10, 36, and 39 are labeled N; the spheres containing 11, 13, and 14 are labeled O; the alternate spheres with dark colors are labeled C).

Molecule shape, electrical structure, and associated characteristics can all be altered by the presence of a solvent. The effects of the solvent were demonstrated using deprotonated $(PAA)^{Iso}$, $(AnB56)^{Iso}$, and $(PAA+AnB56)^{HB/Iso}$, additionally to linked systems where a dye molecule (AnB56)Iso and one or two ethanol molecules form hydrogen bond. (Fig. 1). The geometrical and electrical structures are also examined.

3. Results and Discussion

3.1. Preparation of hybrid blend organic dye $(PAA+AnB56)^{HB}$

The reaction of anthraquinone dye (disperse blue 56 dye) (AnB56) with polyacrylic acid (PAA) was carried out at 120 ^{o}C to yield the hybrid blend organic dye $(PAA+AnB56)^{HB}$ without problems. The reaction was outlined in (Scheme1). FT-IR, ^{1}H-NMR, and UV-Vis absorption spectra were used to characterize the produced hybrid blend organic dye.

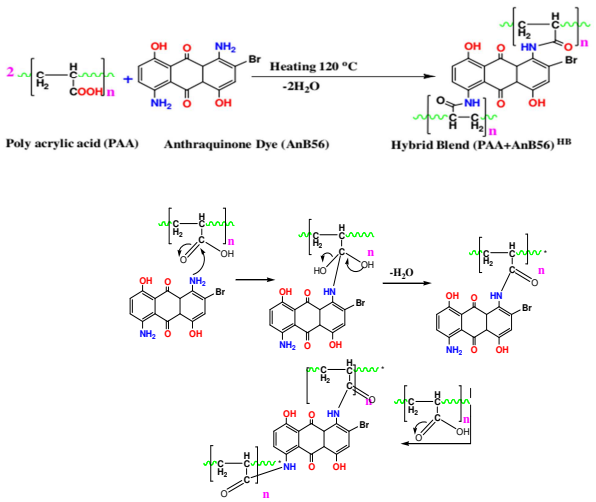

Scheme 1: The synthesis of the hybrid blends organic dye $(PAA+AnB56)^{HB}$

3.2. [1]H-NMR Analysis:

Applying [1]H-NMR analysis to the hybrid blend organic dye (PAA+AnB56)HB characterization procedure is one method of directly viewing the chemical environment of bound hydrogen. Peaks δ = 1.5 -1.8 ppm (doublet, 2H) and δ = 2.3 -2.5 ppm (triplet, 1H) for acrylic proton -CH2-CH- in the backbone at the repeating unit are visible in the [1]H-NMR spectrum data for (PAA+AnB56)HB, broad peak multiplet at downfield region indicating aromatic rings of anthraquininemoiety. (Fig. 2).

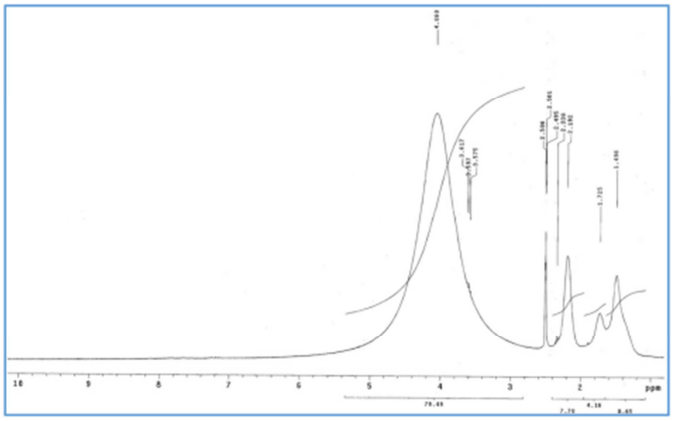

Figure 2: [1]H-NMR spectra of the hybrid blend organic dye (PAA+AnB56)^{HB}

PAA (Poly(acrylic acid)) NMR Spectrum

Poly(acrylic acid) is a simple polymer made from acrylic acid (CH2=CHCOOH) monomers. In the NMR spectrum, you would typically observe the following:

Proton NMR ([1]H NMR):

δ ~ 5.5–6.5 ppm: This region corresponds to the -CH=CH2 (vinyl) protons of the acrylic acid monomer, δ ~ 1.8–2.0 ppm: Methylene protons (-CH_2) next to the carboxyl group, δ ~ 2.2–2.6 ppm: Methylene group adjacent to the -COOH group.

δ ~ 10.5–12.0 ppm: This broad peak represents the -COOH (carboxylic acid) protons in the polymer.

Carbon NMR ([13]C NMR):

δ ~ 170–180 ppm: Carbonyl carbon (C=O) in the carboxylic acid group (-COOH), **δ ~ 40–50 ppm**: Methylene carbon next to the carboxyl group (-CH2COOH), **δ ~ 120–140 ppm**: Carbon of the double bond in the polymer backbone.

NMR spectrum of AnB56 (Anthraquinone-based compound, assumed to be a hybrid polymeric dye)

For a hybrid polymeric dye based on anthraquinone (AnB56), the NMR spectrum would contain peaks indicative of the anthraquinone structure and any polymeric or other functional groups introduced. Some general features you may find include:

Proton NMR ([1]H NMR):

δ ~ 6.5–8.5 ppm: Aromatic protons from the anthraquinone ring system (typically multiple peaks due to the symmetrical structure of the anthraquinone molecule), δ ~ 3.5–5.0 ppm: Protons attached to the polymer backbone if it's a copolymer with ethylene glycol or other monomers.δ ~ 2.0–2.5 ppm: Methylene protons (-CH2) near functional groups (like ester or amide linkages) if the polymer is hybridized with other units.

Carbon NMR ([13]C NMR):

δ ~ 180–190 ppm: Carbonyl carbons from ester/amide groups or the anthraquinone core.

δ ~ 120–140 ppm: Aromatic carbons in the anthraquinone structure.δ ~ 40–50 ppm: Methylene carbons from the polymeric backbone or functional groups attached.

3.3. The FT-IR Analysis:

FTIR Spectrum of PAA (Poly (acrylic acid))

Poly(acrylic acid) has a simple structure, and the FTIR spectrum reflects key functional groups of acrylic acid monomers and the polymer. Here are the main absorption bands you would expect:

Broad peak around 3200–3400 cm^{-1}: This broad absorption is due to the O-H stretch of the carboxylic acid groups (-COOH). This band may also exhibit some broadening due to hydrogen bonding in the polymer.C=O Stretch (carboxyl group): Around 1700–1725 cm^{-1}, you'll observe a strong C=O stretching band corresponding to the carboxyl group (-COOH). The bond C-O Stretch (carboxyl group): A band between 1200–1300 cm^{-1} will correspond to the C-O stretching vibration of the carboxyl group.C-H Stretch: The methyl (-CH_3) and methylene (-CH_2-) groups of the polymer backbone will show characteristic C-H stretches in the range 2800–3000 cm^{-1}.

FTIR Spectrum of AnB56 (Anthraquinone-based Hybrid Polymeric Dye)

Assuming AnB56 is an anthraquinone-based dye that has been polymerized or functionalized, the FTIR spectrum would show peaks characteristic of both the anthraquinone structure and the polymeric or additional functional groups. Below are key regions you might observeC=O Stretch (Carbonyl): Around 1700–1725 cm^{-1}, you'll see a strong C=O stretching absorption from either the anthraquinone carbonyl groups or any ester/amide linkages in the polymer.Aromatic C=C Stretch: Anthraquinone contains an aromatic ring, so you'll see characteristic C=C stretching bands around 1450–1600 cm^{-1} due to the aromatic systems in the anthraquinone.C-H Bending (Aromatic): Bands around 700–900 cm^{-1} typically correspond to out-of-plane C-H bending in the aromatic rings.Aromatic C-H Stretch: A medium to strong absorption around 3000–3100 cm^{-1} may appear due to C-H stretching of the aromatic hydrogens.

C-O Stretch (Polymer Backbone): If the polymer is hybridized with another monomer (e.g., polyesters, polyurethanes, etc.), C-O stretching vibrations from the polymeric ester or ether linkages might appear around 1100–1300 cm^{-1}.C-N Stretch (If amide or amine groups are present): If the dye has been functionalized with amide or amine groups, you might observe a C-N stretching band around 1200–1350 cm^{-1}.

Key Differences between PAA and AnB56 FTIR Spectra

PAA will primarily show a strong carboxyl-related stretching band at **1700 cm^{-1}** and a broad **O-H stretch** around **3200–3400 cm^{-1}**.

AnB56 will have several aromatic-related peaks (from the anthraquinone) and a strong carbonyl stretch around **1700 cm^{-1}**, along with characteristic aromatic C-H stretching and bending peaks.

IR spectra show the following bands in cm^{-1}, 3400-3450 cm^{-1}corresponding to OH and NH in anthraquinone Blue 56 dye (AnB56),1650 cm-1 of C=O carbonyl group in quinine structure (Fig. 4a). The FT-IR spectra of hybrid blend organic dye $(PAA+AnB56)^{HB}$ shows broad band at 3200-3600 cm-1due to presence of NH of amide bond in covalent binding between anthraquinone dye and polyacrylic. Moreover, there is a shift in the carbonyl band at 1720 cm-1 –CO-NH- and C=O quinone moiety. Also, 2622-2800 cm^{-1} of C-H aliphatic of CH2-CH- in $(PAA+AnB56)^{HB}$ (Fig. 3b). This explains the covalent binding between Blue 56 dye and polyacrylic acid.

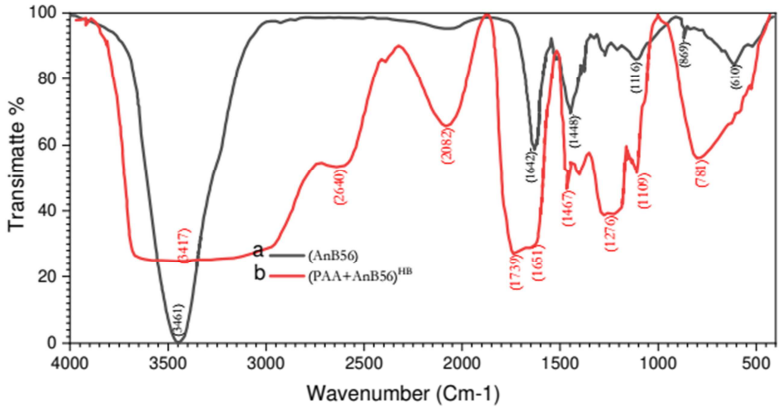

Figure 3: FT-IR spectra of anthraquinone Blue 56 dye (AnB56) and hybrid blend organic dye $(PAA+AnB56)^{HB}$

3.4. The geometrical structure

In order to produce the equivalent isolated molecule of the hybrid mix (PAA+AnB56)HB/Iso structural geometry, the ideal dye (AnB56)Iso with polymer (PAA)Iso is displayed in Fig. 4(a-f). The dihedral angles, bond lengths, and bond angles used are listed in Table 1. Since the predicted distance of 1.501 nm between the C atom in the cyclohexane-1,4-dione and the N atom in the 4-aminocyclohexa-1,3-dien-1-ol is greater than that of comparable dye (see Fig. 4(a-f)), the conjugate bridges of (PAA+AnB56)HB/Iso are slightly longer than those of (AnB56)Iso with polymer (PAA)Iso. The conjugate bridge's coplanar phenyl and tertiary amino groups with the tetrahydroquinoxaline group were also shown. Strong conjugated effects are therefore created.

This conjugation considerably enhances electron transport in conjugated chains. The geometric glyphs of dye sensitizers $(AnB56)^{Iso}$ are likewise comparable.

Deprotonation is a process that can ionize the quaternary ammonium compounds in a solvent. While several non-planar dihedrals were extensively modified, bond lengths and bond angles were only slightly altered in the deprotonated $(AnB56)^{Iso}$, $(PAA)^{Iso}$, and $(PAA+AnB56)^{HB/Iso}$, according to the optimum geometry. This suggests that the deprotonation altered the molecule's electron distribution, which in turn affected the atoms' Coulomb interaction. C2H5OH solute molecules one and

two bind to $(AnB56)^{Iso}$, $(PAA)^{Iso}$, and $(PAA+AnB56)^{HB/Iso}$ using hydrogen bonding, and in order to effect from the solvent on the dye molecule's electrical and geometrical structures $(And)^{Iso}$, these linked complexes were further improved. Fig 2 also included the indications for the hydrogen bond lengths. The MEP ranges of $(AnB56)^{Iso}$ and $(PAA+AnB56)^{HB/Iso}$ matrix in the isolated molecule phase are $-1.273x10^{-2}$ x [MEP] x $8.657x10^{-2}$ and $-1.118x10^{-2}$x [MEP] x $6.412x10^{-2}$, respectively.

Red < brown < blue was determined to be the color order [29-3]. The coupled one and two ethanol molecules' optimal geometries in $(AnB56)^{Iso}$ and $(PAA+AnB56)^{HB/Iso}$ suggest that in these two complexes, the changes in bond angles and dihedrals are more significant than the changes in bond lengths. It follows that bond lengths are less sensitive to charging dispersion as opposed to bond angles and dihedrals. The stereo effect resulting from electron dispersion influenced bond angles and dihedrals, whereas localized contact dominated bond lengths.

As shown in Fig. 6, the ΔE_g^{Opt} values for $(AnB56)^{Iso}$, $(PAA)^{Iso}$, and $(PAA+AnB56)^{HB/Iso}$ were reliant on the disparity between HOMO and LUMO using the TD-DFT/DMOl[3] approach. Two properties that are crucial for the analysis of complexes utilizing the fragment molecular orbital approach (FMOs) technique are the HOMO and LUMO computations. These parameters are applied in simulations of quantum chemistry.

Table 1 shows the computed energy values for E_{HOMO}, $E_{LUMO}$and ΔE_g^{Opt}. The formulae $(\mu = (E_{HOMO} + E_{LUMO})/2), (\chi = -\mu)$, $(\eta = (E_{LUMO} - E_{HOMO})/2)$, $(S = 1/2\eta)$, $(\omega = \mu 2/2\eta)$, ($\sigma = 1/\eta$) and $(\Delta N_{max} = -\mu/\eta)$ are utilized to ascertain electronegativity (χ), softness (σ), potential (μ), global softness (S), global hardness (η), global softness (S), global hardness (η), the maximum amount of electronic charge (ΔN_{max}) and global electrophilicity index (ω),[21-2]. The negative levels of E_{HOMO} and E_{LUMO} energies in their purified form are what indicate the stability of ($(AnB56)^{Iso}$, $(PAA)^{Iso}$, and $(PAA+AnB56)^{HB/Iso}$. One important quantum chemical feature that the device calculates when it gains energy stability by obtaining an extra electrical charge [20].

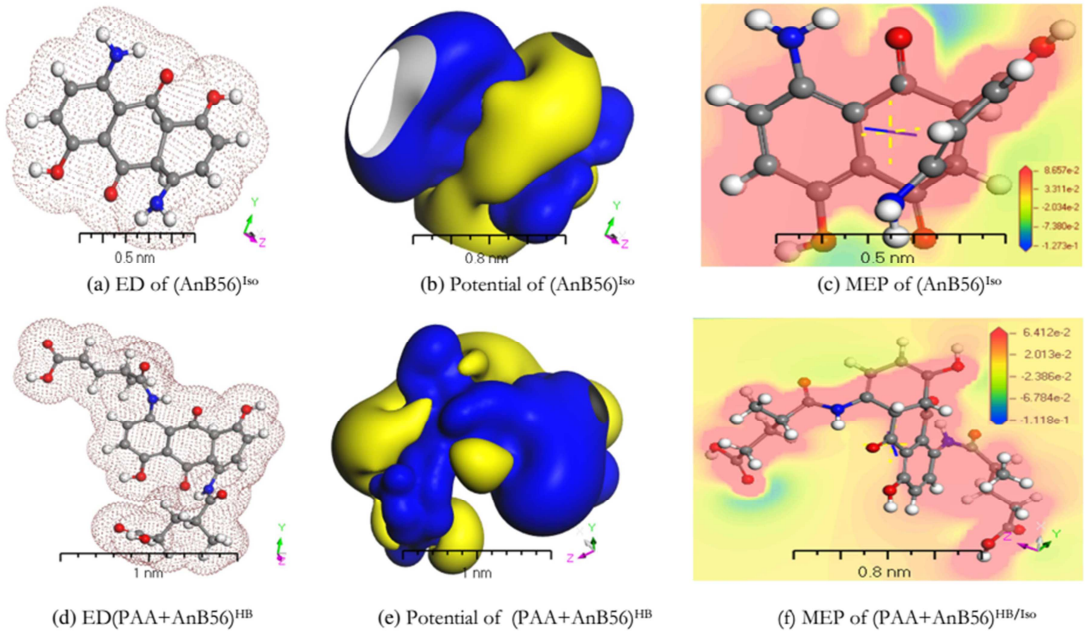

(a) ED of $(AnB56)^{Iso}$ (b) Potential of $(AnB56)^{Iso}$ (c) MEP of $(AnB56)^{Iso}$

(d) ED$(PAA+AnB56)^{HB}$ (e) Potential of $(PAA+AnB56)^{HB}$ (f) MEP of $(PAA+AnB56)^{HB/Iso}$

Figure 4(a, f): Structural geometry of the gas phases $(AnB56)^{Iso}$ and $(PAA+AnB56)^{HB/Iso}$ were optimized using the TD-DFT/DMOl[3] algorithms, respectively.

Table 1: The geometry constant computed for the molecules $(AnB56)^{Iso}$, $(PAA)^{Iso,}$ and $(PAA+AnB56)^{HB/Iso}$.

Molecule	E_{HOMO}	E_{LUMO}	(E_H-E_L)	χ (eV)	μ(eV)	η (eV)	S (eV)	ω (eV)	ΔN_{max}	σ (eV^{-1})
$(AnB56)^{Iso}$	-3.961	-1.981	1.980	2.971	-2.971	-0.990	-0.505	-4.458	-3.001	-1.010
$(PAA+AnB56)^{HB/Iso}$	-4.527	-3.349	1.178	3.938	-3.938	-0.589	-0.849	-13.17	-6.686	-1.698

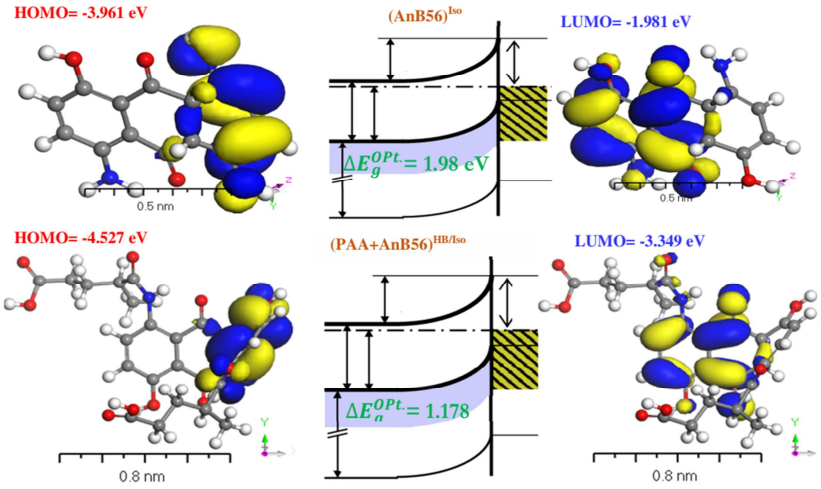

Figure 5: Diagrams showing the energy bands of $(AnB56)^{Iso}$, and $(PAA+AnB56)^{HB/Iso}$.

3.5. Electronic absorption spectra and sensitized mechanism

The adsorption anthraquinonedisperse Blue 56 ($C_{14}H_9ClN_2O_4$) was applied without additional cleaning. To make 1000 p.m. of (AnB56) dye, in 500 milliliters of deionized water, the appropriate amount of dye was weighed out and dissolved. To achieve the desired concentration, the stock solution was diluted. Fresh dilutions were utilized in each experiment. UV-Vis spectra were used to assess the anthraquinone intermediates' and the produced polymeric dyes' adsorption characteristics, and the results were displayed in Fig. 6(a, b). The introduction of the acetyl group in polymeric dye resulted in a hypsochromic shift (blue shift). In the UV-Vis spectra: a) π-π* transitions appear at wavelengths 619 and 639 nm of (AnB56), and $(PAA+AnB56)^{HB}$, respectively. Many dyes and polymer exhibit absorption bands in the UV region due to electronic transitions involving the movement of electrons from a filled π orbital to an empty π* orbital. These transitions are often characterized by intense, sharp peaks.

b) n-π* transitions appear at wavelengths 294 and 288 nm of (AnB56), and $(PAA+AnB56)^{HB}$, respectively: Dyes and polymer containing atoms with lone pairs of electrons (such as nitrogen or oxygen) can undergo n-π* transitions. These transitions involve the excitation of an electron from a non-bonding orbital (n) to an empty π* orbital. n-π* transitions generally occur at longer wavelengths, in the visible region, and are typically broader and less intense compared to π-π* transitions.

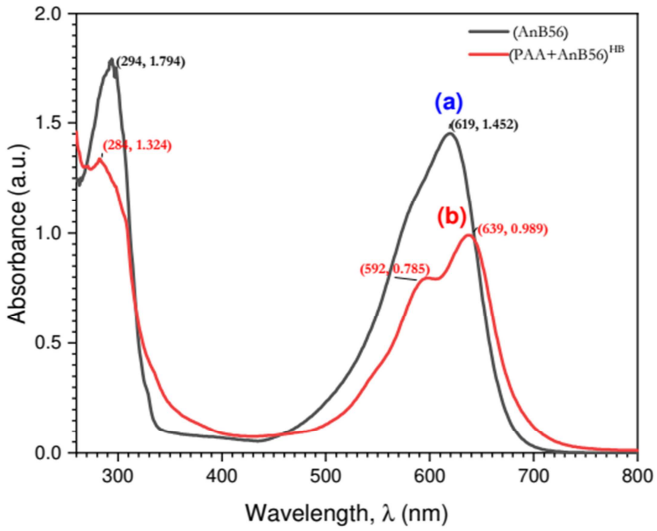

Figure 6: UV-Vis spectra of anthraquinone dye (AnB56) and the hybrid blend $(PAA+AnB56)^{HB}$

The dyes $(AnB56)^{Iso}$ and $(PAA+AnB56)^{HB/Iso}$ in the ethanolic solution exhibit the following UV–vis spectra:

The wavelength of the absorption band's center was 312 and 375 for the first peak and 448 and 496 for the second peak, respectively (Shalaby et al. 2022). The 30 singlet-singlet transitions with the lowest spin-allowed were considered when performing Electronic absorption spectra in vacuum and solvent by TD-DFT computations in order to recognize transitions in electronic systems. Three types of hybrid functionals B3LYP, MPW1PW91, and PBE1PBE in a solvent and two types of hybrid functionals PBE1PBE and B3LYP in a vacuum were used to determine the spectrum. These computations were carried out with B3LYP's optimized geometry. Every transition in the UV–vis spectrum simulation is thought to have a Gaussian distribution. Fig. 7 shows the computed results.$(AnB56)^{Iso}$ and $(PAA+AnB56)^{HB/Iso}$ electronic absorption spectra can be calculated with the hybrid functionals PBE1PBE and MPW1PW91 instead of B3LYP. The computed line form and relative intensity correlate well with the experimental data.The TD-DFT results demonstrate a considerable red shift Compared to the outcomes of the experiment [1], with a solvent's degree of red shift being greater than a vacuum's. Comparable outcomes are likewise obtained by a number of dye sensitizers [40-28]. The difference between the TD-DFT calculations and the experiment could be explained by DFT and solvent effects [31]. In spite of this disparity,the spectral features are explained by the TD-DFT computations due to the qualitative agreement of line shape and relative intensity when compared to the experiment.

The corresponding MO characteristics are analyzed to get microscopic information regarding electronic transitions. Since absorption in the visible and near-UV regions is the most crucial for photo-to-current conversion, Table 1 only includes the singlet →singlet transitions of absorption bands with an oscillator strength more than 0.01 and a wavelength greater than 300 nm. The isodensity plots of the frontier MOs $(PAA+AnB56)^{HB/Iso}$ and $(AnB56)^{Iso}$ are shown in Fig. 7. Transitions of electrons from HOMO-dominated initial states to LUMO-dominated end states produce the absorption bands between 448 and 469 nm.In the phenyl groups, the LUMO π-orbital is contained.The quaternary ammonium group through diphenyl is what makes up the HOMO π*-orbital, which is delocalized (α) throughout the entire molecule. In the case of the near-UV absorption bands, the final states consist of LUMO, while the starting states consist of an orbital mostly connected with MO (HOMO)[16]. Typical π-π* transitions may be seen in the visible and near-UV absorption zones of $(AnB56)^{Iso}$ and $(PAA+AnB56)^{HB/Iso}$, according to the previous investigation of transitions and MOs.

Moreover, the transition with the lowest excited energies does not result in an effective charge-separated state, except for the transitions that are mostly supplied by HOMO→LUMO. Other transitions' final states are mainly linked to MOs localized in electron acceptor groups, while their initial states are mainly linked to MOs localized in electron donor groups.This suggests that the excitations lead to states that are separated in charge, implying that the absorptions are the product of photoinduced electron transfer processes. Because the triphenyl group is notably connected to all of the HOMOs, it is the primary chromophore that helped photo-to-current conversion processes become more sensitive, and it should promote electron injection from the semiconductor surface's excited state[9].

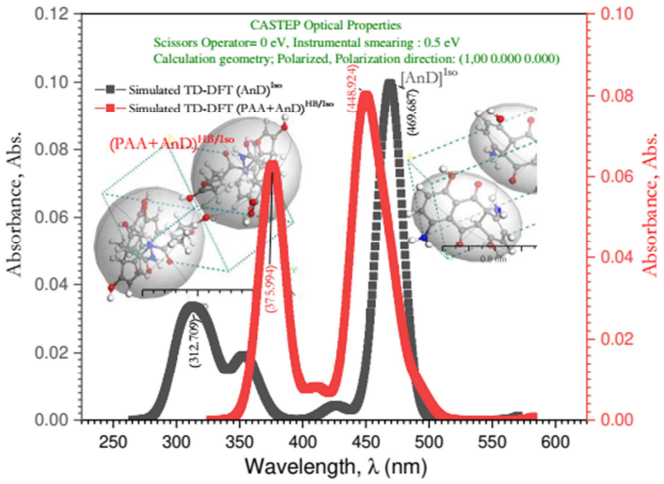

Figure 7: electronic spectra of $(AnB56)^{Iso}$ and $(PAA+AnB56)^{HB/Iso}$ were computed using the TD-DFT/DMOl[3] algorithms.

3.6. Dyeing of polyester fiber (PET) fiber with anthraquinone dye and hybrid blend organic dye.

3.6.1. Dyeing of PET fiber with anthraquinone blue dye$(AnB56)^{Iso}$

Dyeing PET with $(AnB56)^{Iso}$was carried out as described in the experimental part. The dyed PET fabric was evaluated using UV-Vis Spectrophotometer (color matching system) and the result showed that :$L^* = 44.3, a^* = 44.3, and\ b^* = 44.3$

3.6.2. Dyeing of PET fiber with hybrid blend organic dye(PAA+AnB56)$^{HB/Iso}$

Prepared hybrid blend dye was used as prepared to dye PET according to the method described for dyeing the PET with anthraquinone monomeric dye. The UV-Vis spectrophotometer was employed to evaluate the dyed PET fabric and the result showed that: $L^* = 2.6.96, a^* = 3.78, and\ b^* = 39.53$

3.6.3. Comparison of color dyeing with anthraquinone dye and hybrid blend organic dye.

To show the advantages of the hybrid blend organic dye(PAA+AnB56)$^{HB/Iso}$ over the anthraquinone blue dye(AnB56)^{Iso}, a color matching system (UV-visible spectrophotometer) was used to evaluate the main differences between the PET fabric dyed with (AnB56)^{Iso} and (PAA+AnB56)$^{HB/Iso}$. Firstly, the PET sample dyed with (AnB56)^{Iso} was measured and saved in the system, then the PET sample dyed with (PAA+AnB56)$^{HB/Iso}$ was exposed to the system to be measured and saved to compare it with the sample dyed with anthraquinone dye. The result showed much better properties for the hybrid blend organic dye than the anthraquinone monomeric dye. The data is summarized in Table 2.

Table 2: The difference between anthraquinone monomeric blue dye and hybrid blend organic dye on the color matching system.

Dyers	L*	a*	b*	H*	
(AnB56)^{Iso}	44.3	-4.69	-36.33	262.64	
(PAA+AnB56)$^{HB/Iso}$	29.96	3.78	-39.5	275.46	
Difference	DL*=-14.34	Da*=8.47	Db*=-3.20	DH*=12.82	DE*=16.96

The data shown in Table 2 reflects the improvement in the hybrid blend organic dye. For example, DL* represents the difference in lightness between the anthraquinone monomeric blue dye and hybrid blend dye and showed a value of (-14) which means that the PET dyed with (PAA+AnB56)$^{HB/Iso}$ is darker in color than that dyed with (AnB56)^{Iso}. The red-green axis is represented by Da*, which has a value of 8.47. This indicates that the PET dyed with the hybrid blend dye is redder than the sample dyed with anthraquinone monomeric dye. Additionally, Db* has a value of -3.20, indicating that it is bluer. Taken together, these differences mean that DE* is darker, redder, and bluer than the two samples.

3.6.4. Study of the sublimation fastness of both dyed PET with anthraquinone dye and hybrid blend organic dye

Sublimation fastness measures the fastness of dyed fabric with heat. The test was carried out for both fabrics dyed with anthraquinone monomeric blue dye and hybrid blend dye. The results obtained are shown in Table 3. From these results, it can be seen that the fastness of the fabric dyed with (PAA+AnB56)$^{HB/Iso}$ is much better than the fabric dyed with (AnB56)^{Iso} 50% improvement in the fastness of the hybrid blend organic dye.

Table 3: The difference between anthraquinone monomeric blue dye(AnB56)^{Iso} and hybrid blend organic dye(PAA+AnB56)$^{HB/Iso}$ by a color-matching system.

Dye	Sublimation test
(AnB56)^{Iso}	2
(PAA+AnB56)$^{HB/Iso}$	3

3.6.5. Study of the washing fastness of both dyed PET with anthraquinone monomeric blue dye and hybrid blend organic dye

Change in shade, or color loss relative to the initial unwashed sample and staining on the multi-fiber sample, is used to evaluate colorfastness to washing. This was summarized in Table 4.

Table 4: The difference in washing fastness between anthraquinone monomeric blue dye(AnB56)^{Iso} and hybrid blend organic dye(PAA+AnB56)$^{HB/Iso}$is measured by a color-matching system.

Dye	washing test
(AnB56)^{Iso}	3
(PAA+AnB56)$^{HB/Iso}$	4

3.7. SEM and EDX

SEM allows high-resolution imaging of material surface morphology and microstructure. SEM examination may reveal the

individual components of Blue 56 dye and polyacrylic acid (PAA). SEM magnifies Blue 56 dye particles. SEM pictures show dye particle size, shape, and distribution, revealing their morphology. Small, unevenly shaped dye particles may reveal their dispersion properties. SEM study of Blue 56 dye with polyacrylic acid may reveal their characteristics and microstructure (Fig. 8). However, sample preparation, imaging conditions, and the Blue 56 dye and polyacrylic acid utilized might affect SEM data.

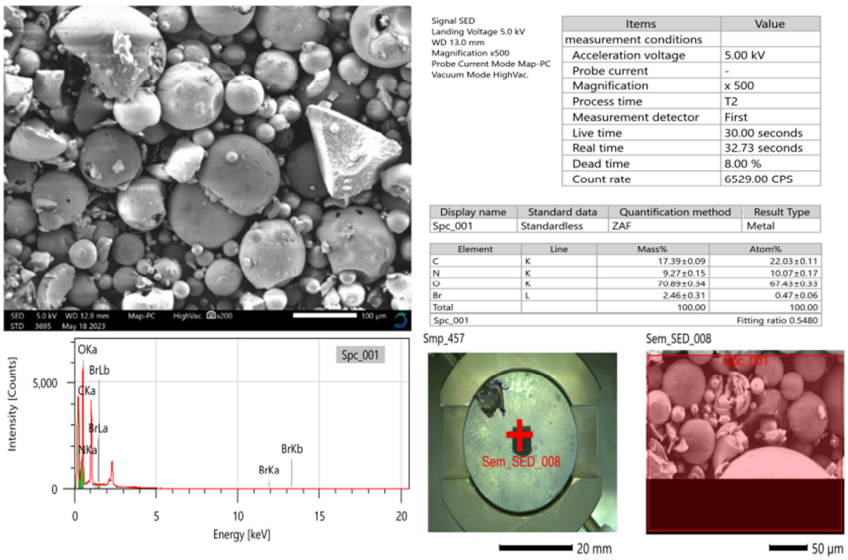

Figure 8: SEM, SEM-SED, and EDX analysis for the disperse blue 56 (AnB56)

The elemental composition of Blue 56 dye and polyacrylic acid (PAA) can be determined using Energy-Dispersive X-ray spectroscopy (EDX). However, without specific sample data, it is not possible to provide exact EDX values for Blue 56 dye and PAA. The elemental composition may vary depending on the specific formulation, impurities, or additives present in the materials. When analyzing the combination of Blue 56 dye and PAA using EDX, the resulting spectrum will contain peaks (O, C, Br, and N) representing the elements found in both materials (Fig. 9). The relative intensities of these peaks can provide information about the composition and distribution of the elements within the dye-polymer complex. This analysis helps confirm the presence of specific elements and assess any potential interactions between the dye and the polymer.

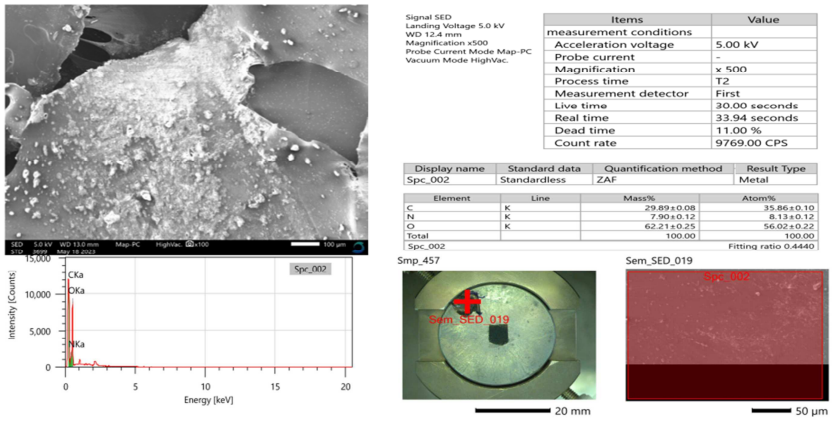

Figure 9: SEM, SEM-SED, and EDX analysis for hybrid blend (PAA+AnB56)^{HB}

4. Conclusion

Blue 56, a polymeric dye based on anthraquinone, was produced with a satisfactory yield. By using FT-IR, 1HNMR, thermal analysis, scanning electron microscopy (SEM), and energy-dispersive X-ray spectroscopy (EDX), the structural andmorphological characteristics of (PAA+AnB56)HB were investigated. The use of these dyes was made possible by their essential properties, which included tremendous depth shade, rapid leveling on the cloth, exceptional fastness to washing and sublimation, and exceptional resilience to extremely high temperatures and chemicals. According to the previously described

research, the shade and fastness properties can be enhanced by enlarging the dye molecule's molecular size via a polymerization procedure. Polymeric colorants were used in the polyester fiber dyeing process to obtain a relatively high depth shade and excellent fastness. EDX: Analysis using energy-dispersive X-ray spectroscopy (EDX) can reveal the Blue 56's elemental makeup.

It can reveal details regarding the dye's incorporation into the polymer matrix, as well as any possible interactions or modifications to the elemental composition in relation to the constituent parts. The observed Uv-Visible spectra and the molecular structure of the materials being tested closely matched the results of the TD-DFT calculations. TD-DFT/DMol3 shows that the isolated hybrid blend molecule for (AnB56)Iso and (PAA+AnB56)HB/Iso has a bandgap of 1.98 and 1.178 eV, respectively.

5. References

[1] Abdel-Aziz, M., H. Maddah, M. S. Zoromba, and A. F. Al-Hossainy, One-dimensional ternary conducting polymers blend with 9.26% power conversion efficiency for photovoltaic devices applications. Alexandria Engineering Journal 66,475-488(2023)

[2] Abdel-Aziz, M. H., E. Z. El-Ashtoukhy, M. Bassyouni, A. F. Al-Hossainy, E. M. Fawzy, S. Abdel-Hamid, and M. S. Zoromba, DFT and experimental study on adsorption of dyes on activated carbon prepared from apple leaves. Carbon Letters 31,863-878 (2021)

[3] Abed-Elmageed, A., M. S. Zoromba, R. Hassanien, and A. Al-Hossainy, Facile synthesis of spin-coated poly (4-nitroaniline) thin film: structural and optical properties. Optical Materials 109 ,110378 (2020)

[4] Adamo, C., and V. Barone, Exchange functionals with improved long-range behavior and adiabatic connection methods without adjustable parameters: The m PW and m PW1PW models. The Journal of chemical physics 108,664-675(1998)

[5] Ahmed, N., S. Nassar, and R. M El-Shishtawy, A novel green continuous dyeing of polyester fabric with excellent color data. Egyptian Journal of Chemistry 63,1-14 (2020)

[6] Al-Hossainy, A. A., Combined Experimental and TDDFT-DFT Computation, Characterization, and Optical Properties for Synthesis of Keto-Bromothymol Blue Dye Thin Film as Optoelectronic Devices. Journal of Electronic Materials 50,3800-3813 (2021)

[7] Alkorta, I., J. Elguero, and A. Frontera, Not only hydrogen bonds: Other noncovalent interactions. Crystals 10,180 (2020).

[8] Augustine, A. K, Synthesis of Nitroso-Based Bis-Azo dyes and their dyeing properties for polyethylene terephthalate and polyamide. Egyptian Journal of Chemistry 63, 3949-3959 (2020)

[9] Barolo, C., M. K. Nazeeruddin, S. Fantacci, D. Di Censo, P. Comte, P. Liska, G. Viscardi, P. Quagliotto, F. De Angelis, and S. Ito, Synthesis, characterization, and DFT-TDDFT computational study of a ruthenium complex containing a functionalized tetradentate ligand. Inorganic chemistry 45,4642-4653 (2006).

[10] Barone, V., and M. Cossi, Quantum calculation of molecular energies and energy gradients in solution by a conductor solvent model. The Journal of Physical Chemistry A 102,1995-2001(1998)

[11] Becke, A. D, Density functional thermochemistry. I. The effect of the exchange only gradient correction. The Journal of chemical physics 96,2155-2160 (1992)

[12] Casida, M. E., C. Jamorski, K. C. Casida, and D. R. Salahub, Molecular excitation energies to high-lying bound states from time-dependent density-functional response theory: Characterization and correction of the time-dependent local density approximation ionization threshold. The Journal of chemical physics 108,4439-4449 (1998)

[13] Couto, R. A. S., S. S. Costa, B. Mounssef, J. G. Pacheco, E. Fernandes, F. Carvalho, C. M. P. Rodrigues, C. Delerue-Matos, A. A. C. Braga, L. Moreira Gonçalves, and M. B. Quinaz, Electrochemical sensing of ecstasy with electropolymerized molecularly imprinted poly(o-phenylenediamine) polymer on the surface of disposable screen-printed carbon electrodes. Sensors and Actuators B: Chemical 290,378-386(2019)

[14] Dawson, J. F, Developments in disperse dyes. Review of progress in coloration and related topics 9,25-35(1978).

[15] Frisch, M., G. Trucks, H. Schlegel, G. E. Scuseria, M. A. Robb, J. R. Cheeseman, J. Montgomery Jr, T. Vreven, K. Kudin, and J. Burant. Gaussian 03, revision c. 02, Gaussian. Inc., Wallingford, CT 4(2004).

[16] Ghosh, S., G. K. Chaitanya, K. Bhanuprakash, M. K. Nazeeruddin, M. Grätzel, and P. Y. Reddy, Electronic structures and absorption spectra of Linkage Isomers of Trithiocyanato (4, 4 ‘, 4 ‘‘-Tricarboxy-2, 2 ‘: 6, 2 ‘‘-terpyridine) Ruthenium (II) complexes: a DFT study. Inorganic chemistry 45,7600-7611(2006).

[17] Hirata, S., and M. Head-Gordon, Chem Phys Lett 314: 291;(b) Hirata S. Head-Gordon M (1999) Chem Phys Lett 302:375.(1999)

[18] Hossain, M. K., M. F. Pervez, M. Mia, A. Mortuza, M. Rahaman, M. Karim, J. M. Islam, F. Ahmed, and M. A. Khan.,Effect of dye extracting solvents and sensitization time on photovoltaic performance of natural dye sensitized solar cells. Results in Physics 7,1516-1523(2017).

[19] Huang, Y., D. Wu, D. Cao, and D. Cheng, Facile preparation of biomass-derived bifunctional electrocatalysts for oxygen reduction and evolution reactions. International Journal of Hydrogen Energy 43,8611-8622(2018).

[20] Kaya, S., L. Guo, C. Kaya, B. Tüzün, I. Obot, R. Touir, and N. Islam.,a. Quantum chemical and molecular dynamic simulation studies for the prediction of inhibition efficiencies of some piperidine derivatives on the corrosion of iron. Journal of the Taiwan Institute of Chemical Engineers 65,522-529(2016).

[21] Kaya, S., B. Tüzün, C. Kaya, and I. B. Obot , Determination of corrosion inhibition effects of amino acids: quantum chemical and molecular dynamic simulation study. Journal of the Taiwan Institute of Chemical Engineers 58,528-535(2016).

[22] Lee, C., W. Yang, and R. G. Parr, Development of the Colle-Salvetti correlation-energy formula into a functional of the electron density. Physical review B 37,785(1988).
[23] Lv, D., J. Cui, Y. Wang, G. Zhu, M. Zhang, and X. Li, Synthesis and color properties of novel polymeric dyes based on grafting of anthraquinone derivatives onto O-carboxymethyl chitosan. RSC advances 7,33494-33501(2017).
[24] Maradiya, H. R., and V. S. Patel, Synthesis, characterization and application of monomeric and polymeric dyes based on N-arylmaleimides. High Performance Polymers 12,335-348(2000).
[25] Maradiya, H. R., and V. S. Patel., Studies of novel monomeric and polymeric azo disperse dyes. Journal of applied polymer science 84,1380-1389(2002).
[26] Maradiya, H. R., and V. S. Patel, N-arylmaleimide based monomeric and polymeric dyes for cellulose triacetate fiber. International Journal of Polymeric Materials 52,119-131(2003)
[27] Miehlich, B., A. Savin, H. Stoll, and H. Preuss, Results obtained with the correlation energy density functionals of Becke and Lee, Yang and Parr. Chemical Physics Letters 157,200-206.(1989).
[28] Mitchla, S., F. Patel, and G. Malik, Synthesis and characterization of monoazo pyrazolone dyes based on 1, 3, 4-thiadiazole and their dyeing performance on polyester fabric. J Ultra Chem 14,8-13(2018).
[29] Mohamed, N. S., S. M. Ibrahim, M. M. Ahmed, and A. F. Al-Hossainy, Removal of toxic basic fuchsin dye from liquids by antibiotic azithromycin using adsorption, TD-DFT calculations, kinetic, and equilibrium studies. Industrial & Engineering Chemistry Research 62,4312-4327(2023).
[30] Mori-Sanchez, P., Q. Wu, and W. Yang, Accurate polymer polarizabilities with exact exchange density-functional theory. The Journal of chemical physics 119,11001-11004(2003).
[31] Mu, B., W. Li, and Y. Yang, Reactive tendering: mechanism and solutions. Cellulose 26,5769-5781(2019)
[32] Onozawa-Komatsuzaki, N., O. Kitao, M. Yanagida, Y. Himeda, H. Sugihara, and K. Kasuga,Molecular and electronic ground and excited structures of heteroleptic ruthenium polypyridyl dyes for nanocrystalline TiO 2 solar cells. New Journal of Chemistry 30,689-697(2006).
[33] Patel, D. R., N. B. Patel, B. M. Patel, and K. C. Patel, Synthesis and dyeing properties of some new monoazo disperse dyes derived from 2-amino-4-(2′, 4′-dichlorophenyl)-1, 3 thiazole. Journal of Saudi Chemical Society 18,902-913(2014)
[34] Perdew, J. P., K. Burke, and M. Ernzerhof, Perdew, burke, and ernzerhof reply. Physical Review Letters 80,891(1998).
[35] Radei, S., F. J. Carrión-Fité, M. Ardanuy, and J. M. Canal, Thermodynamic and kinetic parameters of polyester dyeing with Disperse Blue 56 using bio-based auxiliaries and co-solvent microemulsion. Textile research journal 90,523-536(2020)
[36] Shalaby, M. G., A. F. Al-Hossainy, A. M. Abo-Zeid, H. Mobark, and Y. A.-G. Mahmoud, Combined Experimental Thin Film, DFT-TDDFT Computational Study, structure properties for [FeO+ P2O5] bio-nanocomposite by Geotrichum candidum and Environmental application. Journal of Molecular Structure 1258,132635(2022).
[37] Sharma, J., S. Sharma, and V. Soni, Classification and impact of synthetic textile dyes on Aquatic Flora: A review. Regional Studies in Marine Science 45,101802 (2021).
[38] Shekarriz, M., and F. Haji Aliakbari, Chemistry of Polymeric Textile Dyes. Basparesh 3,69-76(2013).
[39] Stratmann, R. E., G. E. Scuseria, and M. J. Frisch, An efficient implementation of time-dependent density-functional theory for the calculation of excitation energies of large molecules. The Journal of chemical physics 109,8218-8224(1998).
[40] Tolba, M., M. Sayed, S. Abdel-Raheem, T. Gaber, A. El-Dean, and M. Ahmed, Synthesis and spectral characterization of some new thiazolopyrimidine derivatives. Current Chemistry Letters 10,471-478(2021).
[41] Xu, Y., W.-K. Chen, M.-J. Cao, S.-H. Liu, J.-Q. Li, A. I. Philippopoulos, and P. Falaras, A TD-DFT study on the electronic spectrum of Ru (II) L2 [L= bis (5′-methyl-2, 2′-bipyridine-6-carboxylato)] in the gas phase and DMF solution. Chemical physics 330,204-211(2006).
[42] Zoromba, M. S., H. Maddah, M. Abdel-Aziz, and A. F. Al-Hossainy, Physical structure, TD-DFT computations, and optical properties of hybrid nanocomposite thin film as optoelectronic devices. Journal of Industrial and Engineering Chemistry 112,106-124 (2022).
[43] Maradiya, H. R., and V. S. Patel., Disperse dyes based on 2-aminothiazole derivatives for polyester. Bull Chem. Technol. Macedonia 21,57-64.(2002)